Oxidation-Active Flavin Models: Oxidation of α-Hydroxy Acids by Benzo-dipteridine Bearing Metal-Binding Site in the Presence of Divalent Metal Ion and Base in Organic Solvents

Hideaki Ohshiro,[†] Keita Mitsui,[†] Nobuyuki Ando,[†] Yoichi Ohsawa,[†] Wataru Koinuma,[†] Hirobumi Takahashi,[†] Shin-ichi Kondo,[†] Tatsuya Nabeshima,[‡] and Yumihiko Yano*,[†]

Contribution from the Department of Chemistry, Gunma University, Kiryu, Gunma 376-8515, Japan and the Department of Chemistry, University of Tsukuba, Tsukuba, Ibaraki 305-8571, Japan

Received March 14, 2000

Abstract: The oxidizing ability of benzo-dipteridine bearing a bipyridin-6-ylmethyl moiety (**4**) was found to be increased with Zn^{2+} by ∼10^3-fold for sulfite addition in MeOH and ∼10^2-fold for oxidation of an NADH model in MeCN. It was found for the first time that **4** is able to oxidize α-hydroxy acids to α-keto acids in the presence of a divalent metal ion such as Zn^{2+}, Co^{2+}, and Ni^{2+} and an amine base in MeCN or *t*-BuOH, whereas benzo-dipteridine having a bipyridin-5-ylmethyl moiety (**3**) is unable to oxidize them under the same conditions. The oxidation reaction was kinetically investigated including the kinetic isotope effect for deuterated mandelic acids (k_H/k_D = 2.1−3.7) and the Hammett plots for substituted mandelic acids (V-shaped plots). In the reaction of α-substituted α-hydroxy acids such as α-methyl mandelic and benzylic acids with **4**, novel oxidative decarboxylation was found to take place, giving acetophenone and benzophenone, respectively. The oxidation mechanism for mandelic acid was proposed to proceed via a ternary complex of **4**·Zn^{2+}·$PhCH(OH)CO_2^-$, in which α-oxyanion of mandelate attacks C(4a)-position of **4** to form an adduct followed by 1,2-elimination to afford benzoyl formate and 2e-reduced **4**. The roles of the metal ion were proposed as follows; (i) activation of **4**, (ii) substrate-binding site, and (iii) activation of the bound α-hydroxy acid by lowering pK_a's of α-OH and α-CH. This is a first example that a flavin model oxidizes α-hydroxy acids in the presence of a metal ion.

Introduction

Flavin coenzymes such as FMN and FAD exhibit diverse redox functions in biological systems, in which manifestation of the functions is modulated through interactions with apoproteins. Although biochemical and chemical investigations on flavoenzymes have been extensively conducted,[1] still much remains to be clarified in molecular levels. Model study has made a significant contribution to mechanistic understanding of flavin catalysis.[2] We considered that oxidation-active flavin mimics are quite useful not only for the mechanistic study but also for exploitation of new flavin-mediated oxidation reactions because the oxidizing ability of conventional flavin mimics reported thus far is fairly weak. We have successfully exploited highly oxidation-active flavin mimics by chemical modification of an isoalloxazine ring.[3] Among them, benzo-dipteridine (**2**), which is ∼10^7 times more reactive than a conventional flavin model for reactions involving nucleophilic attack at the C(4a)-position, is quite useful. It should be noted that the reactivities of the oxidation-active flavin mimics are correlated with their redox potentials in aqueous solution.[3a] By employing **2**, we reported oxidative dealkylation of *N*-nitrosamines (a metabolic model of *N*-nitrosamines),[3c] oxidation of sulfite ion (an APS reductase model),[3d] and oxidation of *o*-aminophenol (an isophenoxazine synthase model).[3f] To construct more sophisticated model systems,[4] the so-called "artificial flavoenzymes", however, pertinent arrangements of reaction-promoting factors, such as a substrate-binding site, a substrate-activating and transition-state stabilizing factors, are necessary. These might be achieved by covalent and noncovalent functionalization of the oxidation-active flavin mimic. Namely, we can introduce a functional group into a benzo-dipteridine skeleton through covalent bonds and also through noncovalent bonds by employing a functionalized flavin receptor which binds the flavin model close to the functional group.[5] We selected a metal ion as the functionality, since some flavoenzymes require a metal ion as a prosthetic group.[6] For example, D-lactate dehydrogenases from bacterial and mammalian sources, which oxidize D-lactate to pyruvate,

* To whom correspondence should be addressed: yano@chem.gunma-u.ac.jp.

[†]Gunma University.

[‡]University of Tsukuba.

(1) (a) Ghisla, S.; Massey, V. *Eur. J. Biochem*. **1989**, *181*, 1−17. (b) Muller, F., Ed. *Chemistry and Biochemistry of Flavoenzymes*; CRC Press, Boston, 1991; Vols. I−III.

(2) (a) Bruice, T. C. *Acc. Chem. Res*. **1980**, *13*, 256−262. (b) Walsh, C. *Acc. Chem. Res*. **1980**, *13*, 148−156. (c) Bruice, T. C. *Isr. J. Chem*. **1984**, *24*, 54−61.

(3) (a) Yano, Y.; Nakazato, M.; Sutoh, S.; Vasquez, R.; Kitani, A.; Sasaki, K. *J. Chem. Res.* **1985**, 404−405. (b) Yano, Y.; Ohshima, M.; Yatsu, I.; Sutoh, S.; Vasquez, R. E.; Kitani, A.; Sasaki, K. *J. Chem. Soc., Perkin Trans. 2* **1985**, 753−758. (c) Yano, Y.; Ikuta, M.; Yokoyama, T.; Yoshida, K. *J. Org. Chem.* **1987**, *52*, 5606−5610. (d) Yano, Y.; Nakazato, M.; Iizuka, K.; Hoshino, T.; Tanaka, K.; Koga, M.; Yoneda, F. *J. Chem. Soc., Perkin Trans. 2* **1990**, 2179−2185. (e) Yano, Y.; Tamura, N. *Synth. Org. Chem*. **1992**, *50*, 899−907. (f) Yano, Y.; Ikuta, M.; Amamiya, Y.; Nabeshima, T. *Chem. Lett*. **1991**, 461−464.

(4) (a) Murakami, Y.; Kikuchi, J.-I.; Hisaeda, Y.; Hayashida, O. *Chem. Rev*. **1996**, *96*, 721−758. (b) Breslow, R. *Acc. Chem. Res*. **1995**, *28*, 146−153.

(5) (a) Kajiki, T.; Tamura, N.; Nabeshima, T.; Yano, Y. *Chem. Lett*. **1995**, 1063−1064. (b) Kajiki, T.; Moriya, H.; Kondo, S.-I.; Nabeshima, T.; Yano, Y. *J. Chem. Soc., Chem. Commun*. **1998**, 2727−2728. (c) Kajiki, T.; Moriya, H.; Hoshino, K.; Kondo, S.-I.; Yano, Y. *Chem. Lett*. **1999**, 378−379. (d) Kajiki, T.; Kuroi, T.; Moriya, H.; Hoshino, K.; Kondo, S.-I.; Nabeshima, T.; Yano, Y. *J. Org. Chem.* **1999**, *64*, 9679−9689.

10.1021/ja0009121 CCC: $20.00
Published on Web 02/27/2001

Chart 1

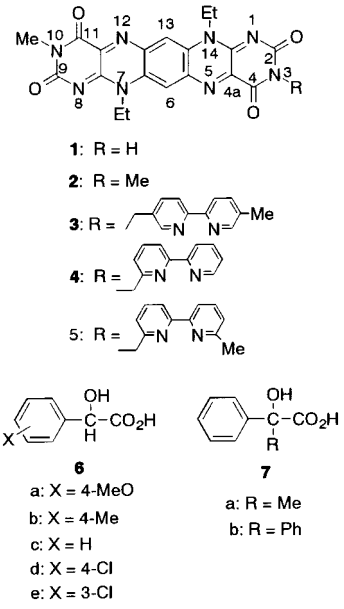

are the only flavoproteins to contain Zn^{2+} in the vicinity of FAD, although the roles of Zn^{2+} are not clearly understood.[7]

We found that **4** is able to oxidize α-hydroxy acids to α-keto acids in the presence of a metal ion and an amine base in organic solvents such as MeCN and *t*-BuOH,[8] whereas **3** is unable to oxidize them; we also found novel oxidative decarboxylation of α-substituted mandelic acids (**7**) such as α-methyl mandelic and benzylic acids by **4**.[9] In this paper, we report the mechanistic study on the oxidation of mandelic acid by **4** in the presence of a metal ion (Zn^{2+}, Co^{2+}, and Ni^{2+}) and Et_3N mainly in MeCN. Flavin models and α-hydroxy acid derivatives employed are shown in Chart 1.

Results and Discussion

Synthesis. BDP_{ox} (**1**) was synthesized in a manner similar to that of **2**[3d] via stepwise condensation of *N*,*N*′-diethyl-*p*-phenylenediamine with 6-chloro-3-methyluracil and 6-chlorouracil. **3**, **4**, and **5** were prepared from **1** and 5-bromomethyl-5′-methyl-2,2′-bipyridine,[10] 6-bromomethyl-2,2′-bipyridine,[11] or 6-bromomethyl-6′-methyl-2,2′-bipyridine[12] in the presence of K_2CO_3 in DMF as outlined in Scheme 1.

Substituted mandelic acids (**6**) were synthesized by hydrolysis of trimethylsilyl ethers of substituted benzaldehyde cyanhydrins, which were prepared from substituted benzaldehydes, potassium cyanide, and chlorotrimethylsilane according to literature procedures.[13]

Scheme 1. Synthetic Route of BDP_{ox}[a]

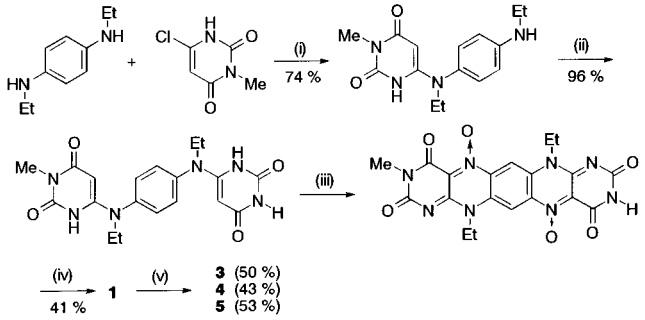

[a] (i) $PhNEt_2$, 1-BuOH, reflux, 20 h, N_2. (ii) 6-Chlorouracil, $PhNEt_2$, 180 °C, 6 h, N_2. (iii) $NaNO_3$/AcOH, H_2SO_4, 90 °C, 6 h, N_2, (iv) DMF, 100 °C, 3 h, N_2. (v) Bromomethyl-2,2′-bipyridines, K_2CO_3, DMF, rt, 4 h, N_2.

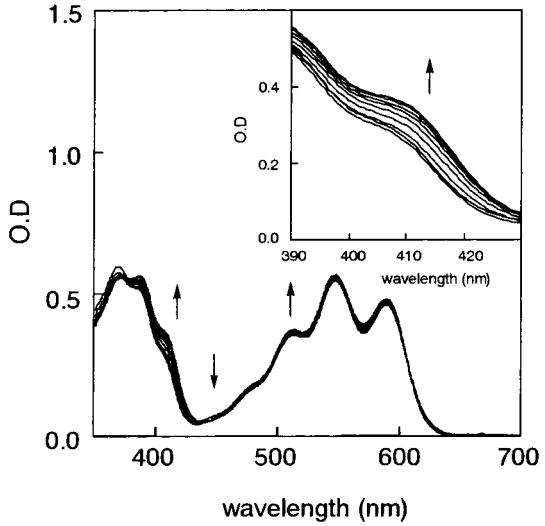

Figure 1. Changes of absorption spectra of 6-bpy-BDP_{ox} upon addition of Zn^{2+}. [**4**] = 3.0×10^{-5} M, [$Zn(NO_3)_2 \cdot 6H_2O$] = $0-6.3 \times 10^{-5}$ M, MeCN, 25 °C.

Metal Binding. The electronic absorption spectra of **4** and **5** were found to shift slightly upon addition of a metal ion in MeCN, whereas such shifts were not observed for **2** and **3** under the same conditions. The spectral changes of **4** upon addition of Zn^{2+} are shown in Figure 1. This indicates that the metal ion bound at the bipyridine moiety of **4** is able to interact with BDP_{ox} skeleton to cause the electronic perturbation. In fact, inspection of CPK molecular models reveals that the interaction of the metal ion bound at the bipyridine moiety with C(2)═O or C(4)═O carbonyl oxygen atoms is geometrically possible only for **4** and **5**. Similar spectral changes were also observed for Co^{2+} and Ni^{2+}. Plots of OD at 412.5 nm vs [M^{2+}] suggest that **4** forms a 1:1 complex with Zn^{2+} and Co^{2+}, whereas a 2:1 complex is formed with Ni^{2+} as shown in Figure 2. However, the spectral changes of **5** upon addition of Ni^{2+} showed a 1:1 complexation.[14]

The metal-binding behavior was also examined by fluorescence spectroscopy. The quenching effect of the metal ions on the fluorescence emission of **4** are shown in Figure 3. The changes of the fluorecence intensities (I/I_o) at 620 nm (excitation at 370 nm) upon addition of the metal ions together with those of **3** and **5** are shown in Figure 4. For **4**, 1:1 complex formation is also suggested for Zn^{2+} and Co^{2+}, and 2:1 complex for Ni^{2+}.

(6) Hattefi. Y.; Stigall, D. L. In *The Enzymes*; Boyer, P. D., Ed.; Academic Press: New York, 1976; Vol. VIII, p 175. Rakagopalan, K. V.; Handler, P. Biological Oxidation; Singer, T. P., Ed.; Interscience: New York, 1968; p 301. Miura, R.; Tojo, H.; Yamano, T. *Chemistry of Metalloproteins*; Ohtsuka, S., Yamanaka, T., Eds.; Kodansha: Tokyo, 1983; p 361.

(7) a) Morpeth, F. F.; Massey, V. *Biochemistry* **1982**, *21*, 1318−1323. (b) Olson, S. T.; Massey, V. *Biochemistry* **1979**, *18*, 4714−4724.

(8) Preliminary communication: Yano, Y.; Mitsui, K.; Ohsawa, Y.; Kobayashi, T.; Nabeshima, T. *J. Chem. Soc., Chem. Commun.* **1993**, 1719−1720.

(9) Preliminary communication: Ando, N.; Ohsawa, Y.; Nabeshima, T.; Yano, Y. *Chem. Lett.* **1996**, 381−382.

(10) Schubert, U. S.; Eschbaume, C.; Hochwimmer, G. *Tetrahedron Lett.* **1998**, *39*, 8643−8644.

(11) (a) Newkome, G. R.; Cupta, V. K.; Frondzek, F. R. *Inorg. Chem.* **1983**, *22*, 171−174. (b) Ziessel, R.; Lehn, J.-M. *Helv. Chim. Acta* **1990**, *73*, 1149−1162.

(12) Rodnguez-Ubis, J.-C.; Alph, B.; Lehn, J.-M. *Helv. Chim. Acta* **1984,** *67*, 2264.

(13) Lee, D. G.; Chen, T. *J. Am. Chem. Soc.* **1993**, *115*, 11231−11236.

(14) Plots of OD at 412.5 nm vs [M^{2+}] followed nicely nonlinear curve fitting for the 1:1 complexation.

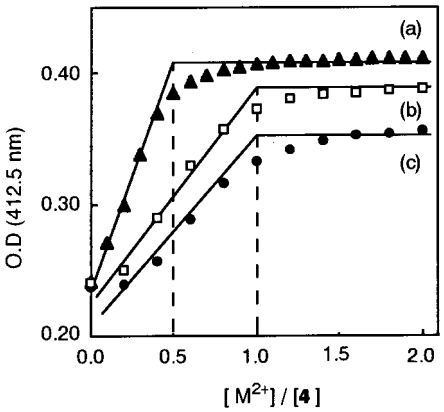

Figure 2. Plots of OD at 412.5 nm vs $[M^{2+}]/[\mathbf{4}]$. $[\mathbf{4}] = 3.0 \times 10^{-5}$ M, (a) Ni^{2+}, (b) Co^{2+}, (c) Zn^{2+}.

For **5**, the gentle decrease of I/I_o with the metal ions implies weaker metal-binding due to 6′-Me group. However, the quenching mode of **5** was complicated.[15] It should be noted that the fluorescence spectra of **2** were little affected upon addition of a metal ion, indicating a free metal ion does not act as a quencher. Complex formation was also examined in MeOH by ESI mass spectroscopy. Formation of the 1:1 complex was also observed for all of the metal ions, and the 2:1 complex was observed only for Ni^{2+} in addition to the 1:1 complex.

By using the data of the absorption spectra, the binding constants for 1:1 complexation were obtained by nonlinear curve fittings (Table 1). The binding ability is in the order of $Ni^{2+} > Co^{2+} > Zn^{2+}$, which is consistent with that of the 1:1 binding constants for 2,2′-bipyridine.[16] The smaller binding constants of **5** compared with those of **4** are explained by steric hindrance of 6′-Me group for metal complexation.[16]

Redox Potentials. Redox potentials were determined by cyclic voltammetry in MeCN−DMF (3:1 v/v). A typical cyclic voltammogram of **4** in the absence of a metal ion is shown in Figure 5, exhibiting two reversible peaks. In the presence of Zn^{2+}, however, it is complicated to analyze the cyclic voltammogram. Namely, the two peaks get close and shift in a positive direction, suggesting that the second cathodic potentials may be more sensitive to the metal ion. A large peak current of the anodic wave was observed, suggesting adosorption of the reduced $\mathbf{4}\cdot M^{2+}$ to the electrode. To avoid the complexity, we examined the effect of Zn^{2+} on the first cathodic potentials (Ep.c). Plots of Ep.c versus $[M^{2+}]/[BDP_{ox}]$ are shown in Figure 6, indicating that Ep.c. values shift abruptly at $[Zn^{2+}]/[BDP_{ox}] = 1$ to reach a saturation. The Ep.c values at the saturation are summarized in Table 2. The Ep.c values of **3**, **4**, and **5** are the same in the absence of Zn^{2+}. In the presence of Zn^{2+}, however, the Ep.c values shift in a positive direction for all BDP_{ox}, and **4** shows a largest shift (+ 0.23 V), suggesting that the oxidation activity of **4** is increased by complexation with the metal ion.

Oxidation Activity. Effects of Zn^{2+} on the oxidation activity of **4** were kinetically examined for addition of sulfite ion and oxidation of an NADH model.

(i) Addition of sulfite ion. We have reported that **2** (λ_{max} 390 and 548 nm) reacts with sulfite ion to form an adduct (λ_{max} 502 nm), which slowly decomposes in a unimolecular manner to give sulfur trioxide and reduced **2** (λ_{max} 620 nm) in aqueous solution.[3d] We have proposed the C(4a)-adduct formation, since **2** facilitates the reactions proceeding a nucleophilic attack at the C(4a)-position. Pseudo-first-order rate constants for **2**, **4**, and **5** were determined by following the absorption increases at 502 nm by stopped-flow technique in MeOH. The effect of Zn^{2+} concentration on the rates is shown in Figure 7a, indicating that **4** shows the largest rate acceleration in the presence of Zn^{2+}. The effect of sulfite-ion concentration on the rates of **4** in the presence of Zn^{2+} is shown in Figure 7b. These results indicate that the reaction proceeds via a complex of **4**, Zn^{2+}, and sulfite ion, allowing us to describe the following reaction scheme and the rate equation (eq 1) by assuming a steady state in [C]. The computed rate constants are listed in Table 3. The computed binding constant (K) in MeOH is smaller than that determined spectrophotometrically in MeCN. This may be explained by the polarity difference of the solvents and by the presence of anionic sulfite ion. It is worthy to note that the reactivity of **5** is much lower than that of **4**. This suggests that 6′-methyl group hinders the complex formation with sulfite ion. As shown in Table 3, the rate acceleration due to Zn^{2+} is 1.2×10^3-fold.

$$\mathbf{4} + Zn^{2+} \overset{K}{\rightleftharpoons} \mathbf{4}\cdot Zn^{2+}$$

$$\mathbf{4}\cdot Zn^{2+} + NaHSO_3 \overset{k_1}{\underset{k_{-1}}{\rightleftharpoons}} C \xrightarrow{k_2} \mathbf{4}\text{-}SO_3^-$$

$$k_{obs} = \frac{k_1 k_2 K[NaHSO_3]_o[Zn^{2+}]_o}{k_1 K[Zn^{2+}]_o[NaHSO_3]_o + (1 + K[Zn^{2+}]_o)(k_{-1} + k_2)} \quad (1)$$

(ii) Oxidation of *N*-benzyl-1,4-dihydronicotinamide (BNAH). The oxidation of BNAH by a flavin model is known to proceed via a hydride (or its equivalent) transfer to N(5)-position of an isoalloxazine ring.[17] Pseudo-first-order rate constants were determined by following the absorption increases of BDP_{red} at 630 nm in MeCN. The concentration effects of Zn^{2+} and BNAH on the rates are shown in Figure 8. The rates for **4** were increased with the increase of $[Zn^{2+}]$, whereas the rates for **2** were little affected. The rates were first-order with respect to [BNAH] regardless of the presence of Zn^{2+}. In the absence of Zn^{2+}, the second-order rate constant (k_2') was 13 M^{-1} s^{-1} These kinetic results allow us to describe the following reaction scheme and rate equation (eq 2). The computed values were as follows: $K = 1.4 \times 10^5$ M^{-1} and $k_2 = 2.6 \times 10^3$ M^{-1} s^{-1}. The K value is fairly consistent with that obtained by spectroscopy, and the rate acceleration due to Zn^{2+} (k_2/k_2') is 2.1×10^2-fold.

$$\mathbf{4} + Zn^{2+} \overset{K}{\rightleftharpoons} \mathbf{4}\cdot Zn^{2+} \xrightarrow{k_2[BNAH]_o} \text{reduced } \mathbf{4}\cdot Zn^{2+} + BNA^+$$

$$k_{obs} = \frac{k_2 K[BNAH]_o[Zn^{2+}]_o}{1 + K[Zn^{2+}]_o} \quad (2)$$

The oxidation activity of **4** can be increased (10^2−10^3-fold) in the presence of Zn^{2+}. This highly oxidation-active system with the metal ion would be used as a model study on metalloflavoenzymes.

Oxidation of α-Hydroxy Acids. D-Lactate dehydrogenases are known to oxidize D-lactate to pyruvate in the presence of Zn^{2+}. We selected the oxidation of α-hydroxy acids by **4** in the presence of a metal ion and tertiary amine in organic solvents. We found that **4** is able to oxidize **6c** to give

(15) Zn^{2+} showed a complicated quenching mode for **3**. I/I_o decreased with the increase of $[Zn^{2+}]$ to reach a mimimum at $[Zn^{2+}]/[\mathbf{3}] = 0.5$ and then the emmision was recovered with further increase of $[Zn^{2+}]$ to generate almost the starting emmision at $[Zn^{2+}]/[\mathbf{3}] = 2$. The quenching mode may be different from that of 6-bpy-BDP_{ox}. We stopped the further study on **3**.

(16) Irving, H.; Mellor, D. H. *J. Chem. Soc.* **1962**, 5222−5237.

(17) (a) Stwart, R.; Norris, D. J. *J. Chem. Soc., Perkin Trans. 2* **1978**, 246−249. (b) Powell, M. F.; Wong, W. H.; Bruice, T. C. *Proc. Natl. Acad. Sci. U.S.A.* **1982**, *79*, 4606−4608. (c) Powell, M. F.; Bruice, T. C. *J. Am. Chem. Soc*. **1983**, *105*, 1014−1021.

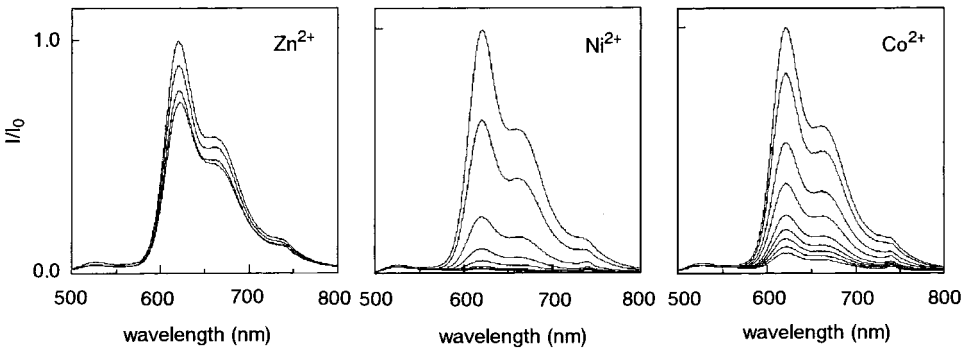

Figure 3. Changes of fluorescence spectra of **4** upon addition of metal ions. Excitation at 370 nm. [**4**] = 5.0×10^{-5}M, [$M(NO_3)_2 \cdot 6H_2O$] = 0−1.0×10^{-4} M, MeCN, 23 °C.

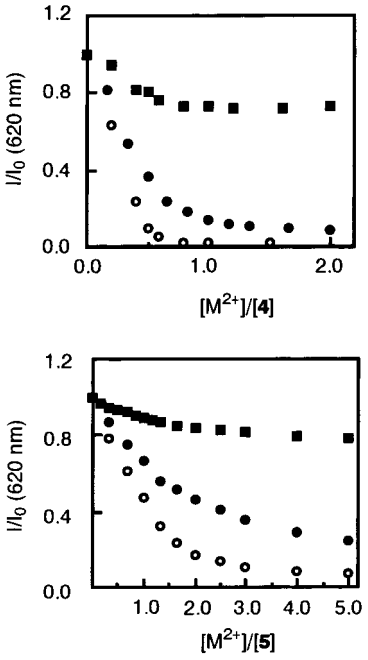

Figure 4. Plots of I/I_o at 620 nm vs [M^{2+}]/[**3**, **4**, or **5**]. (■) Zn^{2+}, (●) Co^{2+}, (○) Ni^{2+}.

Table 1. Binding Constants for 1:1 Complexation in MeCN

BDP_{ox}	M^{2+}	K (M^{-1})
4	Zn^{2+}	3.8×10^5
	Co^{2+}	3.4×10^6
5	Zn^{2+}	3.8×10^4
	Ni^{2+}	4.9×10^6
	Co^{2+}	5.2×10^4

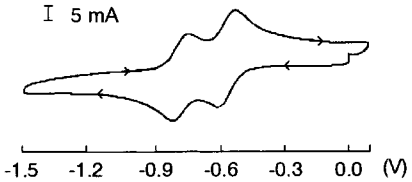

Figure 5. Cyclic voltammogram of **4**. [**4**] = 2.5×10^{-4} M, [TEAP] = 0.1 M, MeCN: DMF = 3:1 (v/v); scan rate 0.5 V/s, 25 °C, N_2.

benzoylformic acid in the presence of the metal ion and amine base in MeCN or *t*-BuOH, whereas **3** and **2** (with 2,2′-bipyridine) are unable to oxidize it, indicating that the positioning of Zn^{2+} is crucial for the oxidation. It is worthy to note that the relative reactivities of $PhCH(OH)CO_2^-$, $PhCH(OH)CO_2Me$, and $MeCH(OH)CO_2^-$ are 20:8:1, implying that the substrate having an anionic moiety and an acidic α-hydrogen shows the larger reactivity.[8] This observation suggests that Zn^{2+} bound at the bipyridine moiety of **4** attracts the anionic substrate to form a ternary complex, in which the acidity of α-OH and α-C−H would be increased because $PhCH(OH)CO_2^-$ is able to coordinate with the metal ion at the CO_2^- and the α-OH groups.[18] In fact, ESI mass spectrum of a mixture of three components showed a molecular ion at 803, which corresponds to *m*/*z* of

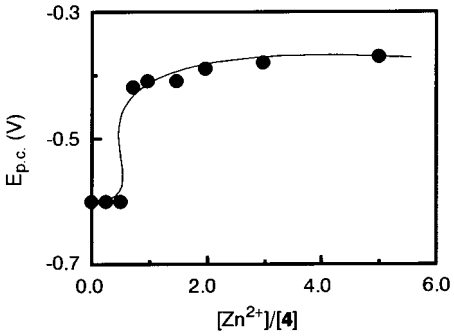

Figure 6. Plots of Ep.c. values vs [Zn^{2+}]/[**4**].

Table 2. Effect of Zn^{2+} On the First Cathodic Potentials of BDP_{ox}'s

BDP_{ox}	$E^o_{p.c.}$ (V)[a]	$E_{p.c.}$ (V)[b]	$\Delta E_{p.c.}$ (V)[c]
2	−0.63	−0.53	+0.10
3	−0.60	−0.48	+0.12
4	−0.60	−0.37	+0.23
5	−0.60	−0.50	+0.10

[a] [Zn^{2+}] = 0 M. [b] [Zn^{2+}] = 1.25×10^{-3} M. [c] $\Delta E_{p.c.} = E_{p.c.} - E^o_{p.c.}$.

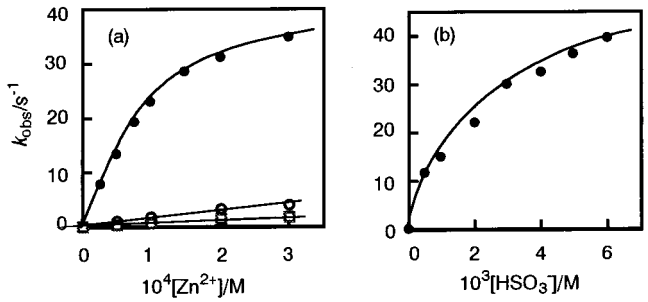

Figure 7. Plot of k_{obs} vs [Zn^{2+}] or [HSO_3^-] for the addition step. [BDP_{ox}] = 1.0×10^{-5} M, MeOH, 25 °C, N_2. (a) [$NaHSO_3$] = 2.5×10^{-4} M. (□) **2,** (●) **4**, (○) **5**. (b) [$Zn(NO_3)_2 \cdot 6H_2O$] = 3.0×10^{-4} M. (●) **4**.

Table 3. Computed Rate Constants

K (M^{-1})	k_2 (s^{-1})	k_2/k_o[a]
1.2×10^3	52	1.2×10^3

[a] k_o: the rate constant without Zn^{2+}. (4.2×10^{-2} s^{-1} at [$NaHSO_3$] = 5.0×10^{-3} M).

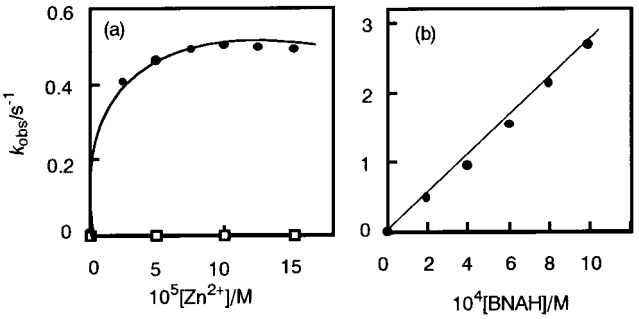

Figure 8. Plots of k_{obs} vs $[Zn^{2+}]$ or [BNAH]. $[BDP_{ox}] = 1.0 \times 10^{-5}$ M, MeCN, 25 °C, N_2. (a) [BNAH] $= 2.0 \times 10^{-4}$ M. (□) **2**, (●) **4**. (b) $[Zn(NO_3)_2 \cdot 6H_2O] = 1.0 \times 10^{-4}$ M. (●) **4**.

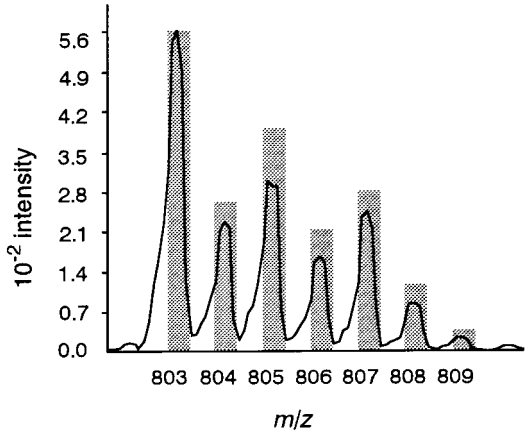

Figure 9. The isotopic pattern of $[\mathbf{4}\cdot Zn^{2+}\cdot PhCH(OH)CO_2^-]^+$. [**4**] = $[Zn(NO_3)_2\cdot 6H_2O]$ = $[Et_3N] = 1.0 \times 10^{-4}$ M, MeCN, 25 °C. Filled bars are the theoretical isotopic pattern of $C_{38}H_{31}N_{10}O_7Zn$.

$[\mathbf{4}\cdot Zn^{2+}\cdot PhCH(OH)CO_2^-]^+$. The isotopic pattern was consistent with the calculated one as shown in Figure 9. Formation of benzoylformic acid (the oxidation product) was detected by HPLC and TLC. This is the first example that a flavin model oxidizes α-hydroxy acids in the presence of a divalent metal ion (D-lactate dehydrogenase model). Thus, we have studied this oxidation in more detail to get an insight into the mechanism and the roles of the metal ions.

(a) Spectroscopic Study. The time course of the spectral changes of **4** with **6c** in the presence of Zn^{2+} and Et_3N in MeCN is shown in Figure 10, showing that the absorption spectrum of $\mathbf{4}\cdot Zn^{2+}$ changes to that of reduced $\mathbf{4}\cdot Zn^{2+}$ via isosbestic points at 410 and 560 nm. As expected, the reduced $\mathbf{4}\cdot Zn^{2+}$ was quite stable toward O_2. Upon addition of 3 N HCl to remove the bound Zn^{2+}, however, the absorption spectrum of **4** was regenerated by O_2 bubbling. This indicates that the present system is unable to be used as a turnover catalytic system under aerobic conditions.

(b) Kinetic Study. Pseudo-first-order rate constants (k_{obs}) were determined by following the absorption increase of reduced $\mathbf{4}\cdot M^{2+}$ at 640 nm in MeCN under anaerobic conditions. The concentration effect of M^{2+} (Zn^{2+}, Co^{2+}, and Ni^{2+}) on the rates showed that the rates increase with the increase of $[M^{2+}]$ to reach maxima and then decrease for all of the metal ions. This is characteristic of the reactions proceeding via a ternary complex in which both the reactants possess metal-binding ability, and the shape of the plots may be dependent on the relative metal-binding abilities of **4** and $PhCH(OH)CO_2^-$. Typical plots for Zn^{2+} and Ni^{2+} are shown in Figure 11. The rate decreases

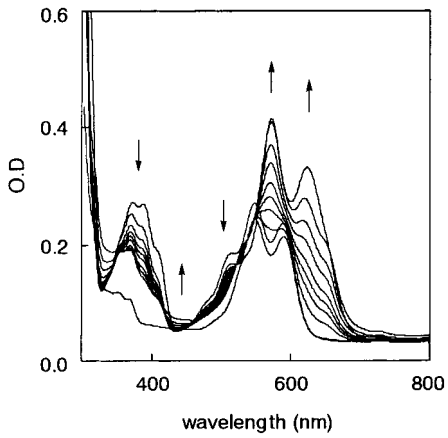

Figure 10. Time courses of spectral changes of **4** in the reaction with **6c**. [**4**] $= 1.0 \times 10^{-5}$ M, [**6c**] $= 2.0 \times 10^{-4}$ M, $[Et_3N] = 6.0 \times 10^{-4}$ M, $[Zn(NO_3)_2\cdot 6H_2O] = 6.0 \times 10^{-4}$ M, MeCN, 25 °C, N_2.

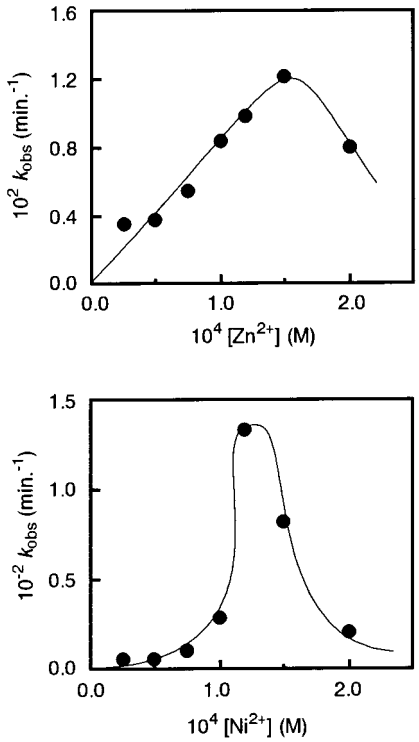

Figure 11. Plots of k_{obs} vs $[Zn^{2+}$ or $Ni^{2+}]$. [**4**] $= 1.0 \times 10^{-5}$ M, [**6c**] $= 2.0 \times 10^{-4}$ M, $[Et_3N] = 6.0 \times 10^{-4}$ M, MeCN, 25 °C, N_2.

in the presence of excess M^{2+} could be explained by the formation of $(\mathbf{6c})_2\cdot M^{2+}$ complex, resulting in the decrease of the concentration of the ternary complex ($\mathbf{4}\cdot M^{2+}\cdot PhCH(OH)CO_2^-$). The rate accelerations are highly dependent on the metal ions. For Ni^{2+}, the rate accelerations are highly sensitive to the metal concentration probably because Ni^{2+} is apt to form a 1:2 complex with the bipyridine moieties and a stronger complex with **6c**, where the concentration of the ternary complex may be highly dependent on the balance of the concentrations of the three components. Meanwhile, carbanion formation at the α-position of carboxylate metal salts is known to be in the order of $Ni^{2+} > Co^{2+} > Zn^{2+}$, which is accounted for by the degree of covalent bond character of the oxygen−metal bond.[18] At the maximum rates in Figure 13, the rate accelerations are: Ni^{2+} (1.0×10^4) > Co^{2+} (80) > Zn^{2+} (1.0). Although the coordination structures of the ternary complexes and the bond character may be responsible for the rates, the reasons for such differences due to the metal ions are not clear at present.

(18) Kovalenko, K. N.; Kazachenko, Kurbatov, V. P.; Kovaleva, L. G. *Russ. J. Inorg. Chem.* **1971**, *16*, 1303−1305.

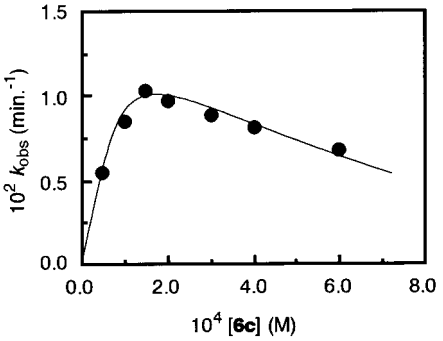

Figure 12. Plots of k_{obs} vs [**6c**]. [**4**] = 1.0×10^{-5} M, [$Zn(NO_3)_2 \cdot 6H_2O$] = 1.2×10^{-4} M, $[Et_3N]_{free} = 6.0 \times 10^{-4}$ M, MeCN, 25 °C, N_2.

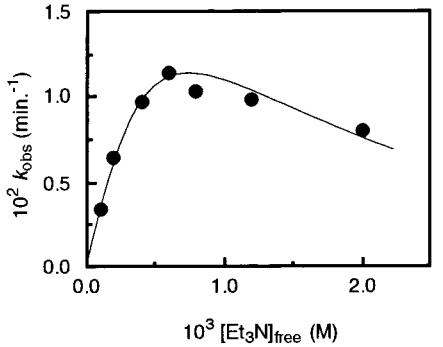

Figure 13. Plots of k_{obs} vs [Et_3N]. [**4**] = 1.0×10^{-5} M, [**6c**] = 2.0×10^{-4} M, [$Zn(NO_3)_2 \cdot 6H_2O$] = 1.2×10^{-4} M, MeCN, 25 °C, N_2.

The activity of **4** was higher than that of **5** for all the metal ions. Namely, the rate enhancements of **4** over **5** were 60-fold for Ni^{2+}, 50-fold for Co^{2+} and 8-fold for Zn^{2+} at their maximam rates. This may be explained by steric hindrance of 6′-Me group for the formation of the ternary complex.

Effects of **6c** and Et_3N concentrations with Zn^{2+} on the rates were examined (Figures 12 and 13).

The rate decreases at higher [**6c**] are due to the formation of a metal complex of mandelate, resulting in the decrease of the ternary complex concentration. The rates increase with the increase of [Et_3N] to reach a maximam, and then decrease gradually with further increase of [Et_3N], indicating the formation of a complex with **4**·M^{2+}·$PhCH(OH)CO_2^-$. The rate decrease at higher concentration of the base may be also explained by the decrease of the concentration of the ternary complex, probably due to competitive coordination of Et_3N to Zn^{2+}.

All of the kinetic data obtained thus far suggest that the metal ion bound at the bipyridine moiety of **4** attracts mandelate to form a ternary complex in which the oxidation takes place.

(c) Mechanism. At least three mechanisms should be taken into consideration: *carbanion mechanism*, *hydride mechanism*, and *addition−elimination mechanism*. Each mechanism involves a spectrum from stepwise to synchronous processes, depending on the timing of bond-breaking and -forming. The carbanion mechanism, in which α-hydroxy acids are concerned, is seen in L-lactate dehydrogenase[20] and mandelate racemase.[21] In mandelate racemase (EC 5.1.2.2), α-carbanion is formed by α-proton abstraction through general acid−base in the presence of a divalent metal ion which plays a crucial role in chelating

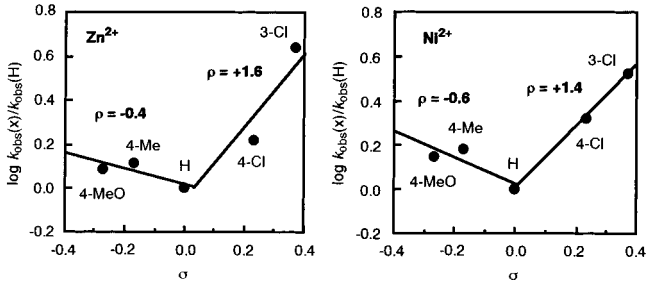

Figure 14. Hammett plots for the oxidation of **6**. [**4**] = 1.0×10^{-5} M, [**6**] = 2.0×10^{-4} M, [Et_3N] = 6.0×10^{-4} M, [$M(NO_3)_2 \cdot 6H_2O$] = 1.2×10^{-4} M, MeCN, 25 °C, N_2.

mandelate and lowering the pK_a of the α-proton. The reasons why the α-proton of mandelate (p$K_a \approx 29$) is abstracted in enzymatic systems are well-investigated.[22] The hydride mechanism, in which abstraction of the α-C−OH proton is coupled with a hydride transfer of α-C−H, is also conceivable.[23] On the other hand, the addition−elimination mechanism comes from the fact that **2** facilitates remarkably the oxidation reactions proceeding through C(4a)-adduct formation, and all of the mechanisms for the oxidation exploited thus far by **2** have been reasonably explained by the addition−elimination mechanism.[3] Since the pK_a of the metal-bound hydroxyl proton is known to be lowered,[24] the α-OH hydrogen of the bound mandelate whithin the ternary complex is abstracted to give the α-oxyanion to undergo a nucleophilic attack at the C(4a)-position to form an adduct followed by base-promoted 1,2-elimination to afford reduced **4**·Zn^{2+} and benzoyl formate. To distiguish these mechanisms, a more detailed study such as substituent effect, kinetic isotope effect, H−D exchange of the α-C−H of mandelate was undertaken.

(i) The Hammett plots were obtained by employing substituted mandelic acids (**6**), and Zn^{2+} and Ni^{2+}. For both of the metal ions, V-shaped plots were obtained as shown in Figure 14, indicating that there are at least two steps in which the sunstituent effect operates inversely. Similar ρ values suggest the oxidation mechanisms to be similar for both of the metal ions.

(ii) The kinetic isotope effects (k_H/k_D) were determined by employing α-deuterated mandelic acids (**6b** and **6c**) in the presence of Zn^{2+} or Ni^{2+}. The deuterated compounds were synthesized from reduction of the corresponding bezoylformic acids[25] by $NaBD_4$ in 1-propanol. The results are summarized in Table 4. The k_H/k_D values indicate that the α-C−H bond-breaking is involved in the rate-determining step.

(iii) No H−D exchange of MA was confirmed under the conditions of [**6c**] = 3.9×10^{-2} M, [$ZnCl_2$] = 3.9×10^{-1} M,

(19) Houghton, R. P. *Metal Complexes in Organic Chemistry*; Cambridge University Press: London; 1979; p 117.

(20) Dubois, J.; Chapmann, S. K.; Mathews, S.; Reid, G. A.; Lederer, F. *Biochemistry* **1990**, *29*, 6393−6400.

(21) Kenyon, G. L.; Gerlt, J. A.; Petsko, G. A.; Kozarich, J. W. *Acc. Chem. Res.* **1995**, *28*, 178−186.

(22) (a) Lin, D. T.; Powers, V. M.; Reynolds, L. J.; Whitman, C. P.; Kozarich, J. W.; Kenyon, G. L. *J. Am. Chem. Soc.* **1988**, *110*, 323−324. (b) Gerlt, J. A.; Kozarich, J. W.; Kenyon, G. L.; Gassman, P. G. *J. Am. Chem. Soc.* **1991**, *113*, 9667−9669. (c) Gerlt, J. A.; Gassman, P. G. *J. Am. Chem. Soc.* **1992**, *114*, 5928−5934. (d) Gerlt, J. A.; Gassman, P. G. *J. Am. Chem. Soc.* **1993**, *115*, 11552−11568. (e) Chiang, Y.; Kresge, A. J.; Popik, V. V.; Schepp, N. P. *J. Am. Chem. Soc.* **1997**, *119*, 10203−10212. (f) Guthrie, J. P.; Kluger, R. *J. Am. Chem. Soc.* **1993**, *115*, 11569−11572.

(23) (a) Yorita, K.; Janko, K.; Aki, K.; Ghisla, S.; Palfey, B. A.; Massey, V. *Proc. Natl. Acad. Sci. U.S.A.* **1997**, *94*, 9590−9595. (b) Mattevi, A.; Vanoni, M. A.; Curti, B. *Curr. Opin. Struct. Biol.* **1997**, *7*, 804−810. (c) Pollegioni, L.; Blodig, W.; Ghisla, S. *J. Biol. Chem.* **1997**, *272*, 4924−4934. (d) Smekal, O.; Reid, G. A.; Chapman, S. K. *Biochem. J.* **1994**, *297*, 647−652.

(24) Kimura, E.; Kodama, Y.; Koike, T.; Shiro, M. *J. Am. Chem. Soc.* **1995**, *117*, 8304−8311. Koike, T.; Inoue, M,; Kimura, E.; Shiro, M. *J. Am. Chem. Soc.* **1996**, *118*, 3091−3099. Ogino, K.; Kashihara, N.; Ueda, T.; Isaka, T.; Yoshida, T.; Tagaki, W. *Bull. Chem. Soc. Jpn.* **1992**, *65*, 373−384.

(25) Baer, E.; Kates, M. *J. Am. Chem. Soc.* **1945**, *67*, 1482−1483.

Table 4. Kinetic Isotope Effects[a]

substrate	k_H/k_D	
	Zn^{2+}	Ni^{2+}
6c	3.7	3.0
6b	2.1	2.4

[a] [**4**] = 1.0×10^{-5} M, [**6**] = 2.0×10^{-4} M, [$Zn(NO_3)_2 \cdot 6H_2O$] = 1.2×10^{-4} M, [Et_3N] = 6.0×10^{-4} M, MeCN, 25 °C, N_2.

[DBU] = 3.6×10^{-1} M in MeOD−MeCN (1:1 v/v)(10 mL) for 24 h at room temperature. It is known that α-C−H of **6c** exchanges very slowly under strongly basic conditions (0.4 M NaOD, 100 °C).[26] Meanwhile mandelate racemase requiring Mg^{2+} undergoes facile H−D exchange in an enzymatic system that is understood by electrophilic catalysis.[27]

For the carbanion mechanism, the ρ value may be positive due to a negative charge that is developed at the α-carbon atom, and for the hydride mechanism, the ρ value may be negative due to a positive charge at the α-carbon atom. Furthermore, the H−D exchange experiment excludes carbanion formation at the α-carbon. We have reported previously that **2** reacts with $PhCH_2O^-$ in $PhCH_2OH$ to give PhCHO,[8] whereas it forms an adduct (530 nm) with *t*-BuO^- in *t*-BuOH.[9] This spectroscopic behavior of the reaction of **2** with alkoxide ions could be explained through the addition−elimination mechanism. Namely, the reaction involves (i) addition step of α-oxy anion at the C(4a)-position, which is favored by electron-donating substituents, and (ii) base-promoted 1,2-elimination step, which is favored by electron-withdrawing substituents. Although the ρ values are small, the V-shaped Hammett plots suggest the two steps are modulated by the electronic property of the substituents. The k_H/k_D values are compatible with any mechanism in which α-C−H bond breaking is involved in the rate-determining step.

Reaction with α-Substituted α-Hydroxy Acids. The results of the reaction with alkoxide ions suggest a possibility that α-hydroxy acids having no α-hydrogen might give an adduct. Thus, α-substituted mandelic acids such as α-methyl mandelic and benzylic acids (**7a** and **7b**), which are unable to be dehydrogenated, were used as the substrate in the reaction with **4** in the presence of Ni^{2+} and DBU in *t*-BuOH. Spectroscopic examination for the reaction of **4** with **7** showed formation of 2e-reduced **4** in both cases, indicating two-electron oxidation of the substrates. Under the conditions of 50 molar excess of the α-hydroxy acids over **4**, the absorption corressponding to the adduct was not observed. Product analysis showed the formation of acetophenone and benzophenone, respectively. No reaction occurred when methyl α-methyl mandelate was used as the substrate. These results clearly indicate oxidative decarboxylation of the α-substituted α-hydroxy acids. The pseudo-first-order rate constants were determined in a manner similar to that for **6**. The results are shown in Table 5 together with the rate constant for the oxidation of **6c**. The decarboxylation step is much slower than the elimination step. It is known that the decarboxylation of carbon acids is facilitated by electron-withdrawing groups at α-carbon.[28] For example, decarboxylation of 2-cyano-2-phenylbutyrate is known to occur at 25 °C in *t*-BuOH.[29] Furthermore, so-called "electron sinks" are necessary to stabilize a carbanion formed by decarboxylation as seen in decarboxylases and their model systems.[30] For example, lactylthiamin is known to be decarboxylated quite easily even in aqueous solution.[31] Thus, an electron-withdrawing moiety must generate at the α-carbon of **7** for the decarboxylation. This could be achieved by the adduct formation as depicted in Scheme 2 (path b). Namely, the electron-withdrawing benzo-dipteridine moiety is introduced at the α-oxygen atom of the substrates through the adduct formation. As a result, the oxidative decarboxylation is facilitated by the fact that the benzo-dipteridine moiety of the adduct acts as a good leaving group. The present oxidative decarboxylation is plausible evidence to support the addition−elimination mechanism.

Table 5. Rate Constants for Oxidation of Mandelic Acid Derivatives[a]

substrate	k_{obs} (min^{-1})	rel. rates
7a	$7.5 \pm 0.3 \times 10^{-2}$	1.0
7b	$6.9 \pm 0.3 \times 10^{-1}$	9.2
6c	1.6×10^{2}	2.1×10^{3}

[a] [**4**] = $1.0 \times 10{-}5$ M, [**6** or **7**] = 5.0×10^{-4} M, [$Ni(NO_3)_2 \cdot 6H_2O$] = 1.0×10^{-4} M, [DBU] = 1.5×10^{-3} M, *t*-BuOH, 25 °C, N_2.

Scheme 2. Reaction Scheme for the Reaction of **4** with α-Hydroxy Acids

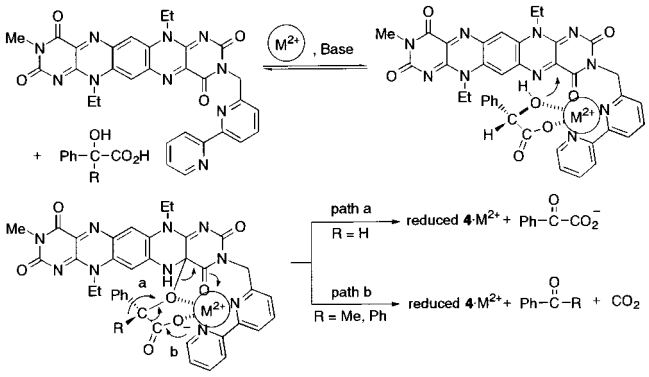

Roles of Metal Ions. The positioning of the metal ion is crucial for the present oxidation. The metal ion bound at the bipyridine moiety of **4** is able to (i) interact with the C(2)═O or the C(4)═O oxygen atom, increasing the oxidation-activity of BDP_{ox} by acting as a Lewis acid, (ii) attract an anionic substrate, and (iii) lower the pK_a's of α-O−H and α-C−H to facilitate both the nucleophilic attack and the successive base-promoted elimination as shown in Scheme 2 (path a).

Conclusions

An oxidation-active flavin mimic bearing a bipyridine moiety (**4**) was found to oxidize α-hydroxy acids to α-keto acids in the presence of a metal ion and amine base in organic solvents, whereas **3** was unable to oxidize them under the same conditions. The oxidation was proposed to proceed through the formation of the ternary complex of **4**, M^{2+}, and α-hydroxy acid, in which the metal-coordinated hydroxyl group attacks the C(4a)-position to form an adduct, followed by base-promoted 1,2-elimination to give reduced **4**·M^{2+} and α-keto acid. When α-substituted α-hydroxy acids (**7**) were used as a substrate, new

(26) Polavarapu, P. L.; Fontana, L. P.; Smith, H. *J. Am. Chem. Soc*. **1986**, *108*, 94−99.

(27) (a) Powers, V. M.; Koo, C. W.; Kenyon, G. L.; Gerlt, J. A.; Kozarich, J. W. *Biochemistry* **1991**, *30*, 9255−9263. (b) Neidhart, D. J.; Howell, P. L.; Petosko, G. A.; Powers, V. M.; Li, L.; Kenyon, G. L.; Gerlt, J. A. *Biochemistry* **1991**, *30*, 9264−9273. (c) Lndro, J. A.; Kallarakal, A. T.; Ransom, S. C.; Gerlt, J. A.; Kozarich, J. W.; Neidhart, D. J.; Kenyon, G. L. *Biochemistry* **1991**, *30*, 9274−9281.

(28) Cram, D. J. *Fundamentals of Carbanion Chemistry*; Academic Press: New York, 1965.

(29) Cram, D. J.; Haberfield, P. *J. Am. Chem. Soc*. **1961**, *83*, 2354−2362, 2362−2367.

(30) O'Leary, M. H. In *Bioorganic Chemistry*; van Tamelen, E. E., Ed.; Academic Press, New York, 1977; Chapter 11, p 259.

(31) Kluger, R.; Chin, J.; Smith. T. *J. Am. Chem. Soc*. **1981**, *103*, 884−888.

oxidative decarboxylation was found to take place, giving the corresponding ketones. It should be noted that it is the first example of the oxidation of α-hydroxy acids by a flavin model. The mechanism could be different from that of D-lactate dehydrogenase, since the present system uses a unique flavin model. However, similar roles of the metal ion are conceivable in native D-lactate dehydrogenases, in which Zn^{2+} is known to be located in the vicinity of FAD.

Experimental Section

^{1}H NMR spectra were recorded on Varian Gemini-200 (200 MHz) or a JEOL JAM α-500 (500 MHz) instrument with chemical shifts from tetramethylsilane. Cyclic voltammograms were recorded on a Hokuto Denko (HA-301, 1B-104) with an X−Y recorder (Riken Electronics F-35). Electronic absorption spectra were recorded on a JASCO Ubset-560 or Shimadzu UV-2200 A spectrophotometer. Stopped-flow rate measurements were performed with Otuka Electronics RA-401 spectrophotometer. Fluorescence spectra were measured on a Hitachi 850 fluorescence spectrophotometer. Melting points are uncorrected. Flash column chromatography was performed by using Wakogel C-200 (silica gel, 70−150 μm, Wako Pure Chemical Co.). Elemental analyses were performed at the Center of Instrumental Analysis of Gunma University. Divalent metal ions used were $M(NO_3)_2 \cdot 6H_2O$. Acetonitrile and DMF were purified by distillation from calcium hydride.

Synthesis of BDP_{ox}. BDP_{ox} (**2**) was supplied from our previous study.[3d] BDP_{ox}(**1**) was prepared by stepwise reactions of *N*,*N*′-diethyl-*p*-phenylenediamine with 6-chloro-3-methyluracil and 6-chlorouracil.

***N*,*N*′-Diethyl-*N*-(3-methyluracil-6-yl)-*N*′-(uracil-6-yl)-*p*-phenylenediamine.** A mixture of *N*,*N*′-diethyl-*N*-(3-methyluracil-6-yl)-*p*-phenylenediamine[32] (3 g, 10 mmol) and 6-chlorouracil (2.3 g, 15 mmol) in *N*,*N*-diethylaniline (3.6 mL) was heated at 180 °C for 1 h under N_2. After cooling, diethyl ether (20 mL) containing a small amount of EtOH was added to crush to pieces. The powdery precipitate was collected by filtration and washed with water (20 mL × 2). Purification was performed by precipitation from acetic acid and diethyl ether to give powder. Yield 2.6 g (96%), mp >300 °C. ^{1}H NMR (200 MHz, DMSO-d_6) δ 1.10 (t, 6H), 3.07 (s, 3H), 3.69 (q, 4H), 4.59 (s, 1H), 4.76 (s, 1H), 7.34 (s, 4H), 9.79(s, 1H), 10.11(s, 1H), 10.43 (s, 1H).

7,14-Diethyl-3-methylbenzo[1,2-g; 4,5-g′]dipteridine-2,4,9,11-(3H,7H,10H,14H)-tetraone (1). A mixture of the above diamine (1.8 g, 4.5 mmol), $NaNO_3$ (3.2 g, 38 mmol), and concentrated H_2SO_4 (0.2 mL) in AcOH (30 mL) was heated at 90 °C for 6 h under N_2. After the mixture cooled, AcOH was evaporated, and the residue was extracted with hot DMF−$CHCl_3$ solution. Di-*N*-oxide was obtained by evaporating the solvent. Without purification, deoxygenation was performed in DMF (10 mL) at 100 °C for 3 h. After this mixture cooled, DMF was evaporated, and diethyl ether (100 mL) was added to give the powder of **1**, which was purified by recrystallization from DMF (violet powder). Yield 0.77 g (41%), mp > 300 °C. UV−vis ($CHCl_3$−DMSO (9:1)). λ_{max} (log ϵ): 370 nm (4.29 M^{-1} cm^{-1}), 553 (4.2). ^{1}H NMR (200 MHz, $CDCl_3$−CF_3CO_2H (5:2 v/v) δ 1.68 (m, 6H), 3.71 (s, 3H), 4.98 (4H, m), 8.92 (s, 1H), 8.95 (s, 1H).

7,14-Diethyl-3-(bipyridin-6-ylmethyl)-10-methylbenzo[1,2-g; 4,5-g′]dipteridine -2,4,9,11-(3H,7H,10H,14H)-tetraone (4). A mixture of **1** (0.20 g, 0.48 mmol), 6-bromomethyl-2,2′-bipyridine[11](0.20 g, 0.8 mmol), and K_2CO_3 (0.20 g, 1.5 mmol) in DMF (150 mL) was stirred for 4 h at room temperature under N_2. After filtration of inorganic salts, DMF was evaporated under reduced pressure, and $CHCl_3$ (200 mL) was added. The $CHCl_3$ layer was washed with water and dried over Na_2SO_4. After evaporating $CHCl_3$, the residue was recrystallized from DMF. Yield 0.12 g (43%), mp > 300 °C. UV−vis ($CHCl_3$-DMF 9:1): λ_{max} (log ϵ) 373 (4.5), 555 (4.5). ^{1}H NMR (200 MHz, $CDCl_3$) δ 1.55 (m, 6H), 3.57 (s,3H), 4.80 (m, 4H), 5.53 (s, 2H), 7.21 (m, 1H), 7.38 (d, J = 7.5 Hz, 1H), 7.69 (t, J = 7.5 Hz, 1H), 7.78 (t, J = 7.5 Hz, 1H), 8.25 (d, J = 7.5 Hz, 1H), 8.33 (d, J = 7.5 Hz, 1H), 8.55 (s, 1H), 8.56 (s, 1H), 8.61 (m, 1H). Anal. Calcd for $C_{30}H_{24}N_{10}O_4 \cdot H_2O$: C, 59.4; H, 4.32; N, 23.09. Found: C, 59.82; H, 4.39; N, 22.72.

3 and **5** were similarly synthesized from **1** and 5-bromomethyl-5′-methyl-2,2′-bipyridine[10] and 6-bromomethyl-6′-methyl-2,2′-bipyridine,[12] **3**. Yield 61%, mp > 300 °C. ^{1}H NMR (200 MHz, $CDCl_3$) δ 1.55 (m, 6H), 2.38 (s, 3H), 3.57 (s, 3H), 4.78 (m, 4H), 5.37 (s, 2H), 7.61 (d, J = 10.0 Hz, 1H), 8.04 (d, J = 10.0 Hz, 1H), 8.27 (d, J = 10.0 Hz, 1H), 8.31 (d, J = 10.0 Hz, 1H), 8.48 (d, J = 10.0 Hz, 1H), 8.54 (s, 1H), 8.56 (s, 1H), 8.90 (s, 1H). Anal. Calcd for $C_{31}H_{26}N_{10}O_4 \cdot H_2O$: C, 59.99; H, 4.55; N, 22.65. Found: C, 60.35; H, 4.63; N, 22.65.

5: yield 54%, mp > 300 °C. ^{1}H NMR (200 MHz, $CDCl_3$) δ 1.56 (m, 6H), 2.68 (s, 3H), 3.57 (s, 3H), 4.80 (m, 4H), 5.53 (s, 2H), 7.17 (d, J = 8.0 Hz, 1H), 7.42 (d, J = 8.0 Hz, 1H), 7.68 (m, 1H), 7.81 (t, J = 8.0 Hz, 1H), 8.13 (d, J = 8.0 Hz, 1H), 8.37 (d, J = 8.0 Hz, 1H), 8.55 (s, 1H), 8.57 (s, 1H). Anal. Calcd for $C_{31}H_{26}N_{10}O_4 \cdot 2H_2O$: C, 58.30; H, 4.73; N, 21.93. Found: C, 58.60; H, 4.96; N, 22.05.

Substituted mandelic acids (**6**) were prepared in fairly good yields according to the literature procedures.[13] Namely, trimethylsilyl ether of substituted benzcyanohydrins, which were prepared from substituted benzaldehydes, potassium cyanide, and chlorotrimethylsilane in the presence of ZnI_2 in MeCN, were hydrolyzed in acidic aqueous solution. **6a**: mp 108−110 °C (benzene) (lit.[13] 106.5−108 °C). **6b**: mp 145−147 °C (benzene) (lit.[13] 145−146 °C). **6d**: mp 117−119 °C (benzene) (lit.[13] 119−121 °C). **6e**: mp 96−97 °C (benzene) (lit.[13] 113.5−115 °C).

Deuterated mandelic acids were prepared by $NaBD_4$-reduction of arylglyoxylic acids,[25] which were prepared by $Pb(CH_3CO_2)_4$- oxidation of the substituted mandelic acids in benzene.[26] The D-contents were determined by comparison with chemical shifts of aryl protons: 86% (**6b**) and 83% (**6c**). The k_H/k_D values were calculated by correction of k_D values; $k_D = (k_{obs} - 0.17k_H)/0.83$ for 83% D-content.

Determination of Redox Potentials. Cyclic voltammetry was carried out using a platinum plate (3 mm in diameter, BAS), Ag/Ag^+ (0.1 M tetraethylammonium perchlorate, TEAP, in MeCN), and platinum wire as working, reference, and counter electrodes in MeCN. A solution of BDP_{ox} (1.0×10^{-3} M in MeCN containing 0.1 M TEAP) and metal ions (12 μL each, 5.02×10^{-2} M in MeCN) was degassed by bubbling N_2 presaturated with MeCN for 20 min. All potentials were measured with scan rate 100 mV s^{-1}. MeCN was purified by distillation from calcium hydride, and TEBP was recrystallized from EtOH−H_2O two times and dried overnight at 100 °C.

Kinetics. (i) Addition of Sulfite Ion. Pseudo-first-order rate constants were determined by following the absorption increases of the adduct at 502 nm in MeOH with a stooped-flow aparatus. Namely, in one reservoir BDP_{ox} (1.0×10^{-5} M: 60 μL of 1.0×10^{-3} M in DMF) and $Zn(NO_3)_2 \cdot 6H_2O$ (30−360 μL of 5.0×10^{-3} M in MeOH) were placed with MeOH (total 3 mL), and $NaHSO_3$ (5.0×10^{-3} M: 30 μL of 1.0 M in H_2O) were placed with MeOH (2.96 mL) in another reservoir. After flowing N_2 in the reservoir, the reaction was started.

(ii) BNAH Oxidation. Psusdo-first-order rate constants were determined by following the absorption increases of BDP_{ox} at 640 nm with a stopped-flow apparatus. In one reservoir, BDP_{ox} (1.0×10^{-5} M: 60 μL of 1.0×10^{-3} M in DMF) and $Zn(NO_3)_2 \cdot 6H_2O$ (30−180 μL of 5.0×10^{-3} M in MeCN) were placed by a microsyringe with MeCN (total 3 mL), and BNAH (2.0×10^{-4} M: 24 μL of 5.0×10^{-2}M in MeCN) was placed with MeCN (2.98 mL) in another reservoir.

(iii) Oxidation of α-Hydroxy Acids. Pseudo-first-order rate constants were determined spectrophotometrically by following the absorption increases of BDP_{red} at 640 nm in MeCN under anaerobic conditions. In a typical run, BDP_{ox} (1.0×10^{-5} M: 30 μL of 1.0×10^{-3} M in DMF) and $Zn(NO_3)_2 \cdot 6H_2O$ (15−120 μL of 5.0×10^{-3} M in MeCN) were placed by a microsyringe in a cell part of a Thunberg cuvette with MeCN, and mandelic acid (2.0×10^{-4} M: 30 μL of 2.0×10^{-2} M in MeCN) was placed in the upper part (the total volume was adjusted to be 3 mL). The solutions were degassed for 30 min at 25 °C by bubbling N_2, prehumidified with MeCN, and just prior to the end, Et_3N (6.0×10^{-4} M: 30 μL of 6.0×10^{-2} M in MeCN) was added quickly. The reaction was started by a quick mixing by up-and-down shaking.

Product Analysis. Formation of benzoyl formate was confirmed by HPLC and TLC analyses. For HPLC, a solution of **4** (1.0×10^{-5}

(32) Yoneda, F.; Koga, M.; Tanaka, K.; Yano, Y. *J. Heterocycl. Chem.* **1989**, *26*, 1221−1228.

M), **6c** (1.0×10^{-4} M), Et_3N (1.1×10^{-3} M), and $Zn(NO_3)_2 \cdot 6H_2O$ (8.0×10^{-5} M) in *t*-BuOH (12 mL, 1% DMF) was stirred for 6 h in the dark under N_2 atmosphere at room temperature. Control experiments were carried out under the conditions of (i) without 6-bpy-BDP_{ox} or (ii) without Zn^{2+}. After evaporation of *t*-BuOH, MeCN (5 mL) was added. This was subjected to HPLC analysis (Wakopak Wakosil II-5C18 column; H_2O/MeCN = 3/40 or Wakopak Wakosil 5C18, 4.6 mm (Ø) × 150 mm, 0.25 mL/min). Formation of benzoyl formate was confirmed on both the column based on retention time. From the control experiments, no formation of benzoyl formate was observed. For TLC, a solution of 6-bpy-BDP_{ox} (1.0×10^{-5} M), MA (1.0×10^{-4} M), $Zn(NO_3)_2 \cdot 6H_2O$ (8.0×10^{-5} M), and Et_3N(1.1×10^{-3} M) in *t*-BuOH (500 mL, 1% DMF) was stirred for 6 h in dark under N_2 atmosphere at room temperature. After evaporation of *t*-BuOH, $CHCl_3$ (5 mL) was added to the residue. Formation of benzoyl formate was confirmed on TLC (Merck, TLC Plate Silica Gel 60 F-60 F-254, MeCN/MeOH = 5/1 v/v, $R_f = 0.33$) yellow-colored spot by spraying 0.1 N HCl solution containing 2,4-dinitrophenylhydrazine.

Acknowledgment. This work was supported in part by Grant-in-Aid for Scientific Research from the Ministry of Education, Science, Sports, and Culture of Japan.

JA0009121